Force Analysis of Statically Balanced Serially Connected Manipulators Using Springs Based on Torque Compatibilities Associated With Accumulative Joint Angles

Chi-Shiun Jhuang
Department of Mechanical Engineering,
National Taiwan University,
Taipei 10617, Taiwan
e-mail: d06522028@ntu.edu.tw

Chia-Wei Juang
Department of Mechanical Engineering,
National Taiwan University,
Taipei 10617, Taiwan
e-mail: f06522638@ntu.edu.tw

Dar-Zen Chen[1]
Department of Mechanical Engineering,
National Taiwan University,
Taipei 10617, Taiwan
e-mail: dzchen@ntu.edu.tw

Force analysis with regard to serial connected manipulators is discussed thoroughly in the past. However, force analysis of statically balanced manipulator using springs has not been widely addressed because spring forces and motions do not share an immediate association. In this article, spring forces are represented as accumulative joint angles of links crossed by springs and attached angles/lengths of springs. Torque equilibrium equations regarding the preconnected joint of a typical link as contributed by gravity force and spring force can be inwardly formed link by link from the end link. Compatibility with the same accumulative joint angle can be formulated under static balance conditions. Hence, spring attachment parameters such as spring stiffness and attachment lengths are constrained by given link properties and spring attachment angles. Thus, spring forces can be determined by a chosen set of stiffness and attached lengths of springs, and the joint reaction force can then be determined. Example figures of 3-degrees-of-freedom (DOFs) manipulators show that joint reaction forces are reduced by 22.6%, 40.1%, and 75.7% at joints 1, 2, and 3, respectively, than those without springs. It is found that besides balancing gravity, the statically balanced manipulator is with lower joint reaction forces. Hence, the manipulator can be more lightweight by using compact joints and links with the same material. Furthermore, the static and dynamic performance of the manipulator can be improved by the effect of reduced joint reaction forces as well. [DOI: 10.1115/1.4056960]

Keywords: spring static balance, joint reaction force, serially connected manipulator, force analysis, mechanism design, robot design, theoretical kinematics

1 Introduction

Analysis of joint reaction forces on joints of serial connected manipulators is discussed in the robotics field already [1–3]. These manipulators are used in industry or manufacture [4], or for assisting users with certain functions [5]. For instance, surgical robot arms such as the daVinci Surgical Robot system assist doctors to do surgeries [6,7]; and exoskeletons such as artificial arms, legs, or trunks help patients with muscular weakness to do their daily activities or rehabilitation [8–10].

To drive the aforementioned manipulators, it usually requires objects that might need a lot of effort to start. Gravity balance is a way to compensate the effect gravity has on the manipulator and to make the operation smoother. One method of achieving gravity balance is to use springs to eliminate the effect of gravity on manipulators [11,12]. Torques on each joint of a static balanced manipulator maintains zero at all times, and the manipulator can stay at any posture. Herder et al. [13,14] and Deepak and Ananthasuresh [15] presented a gravity equilibrator by adding springs to the manipulator to achieve static balance. They focused on the specific design of equilibrator rather than providing systematic methods for the manipulator. Chen et al. [16–18] utilized the stiffness block matrix method to investigate spring configurations and to let a planar or spatial manipulator to achieve static balance. Huysamen et al. and Bortoletto et al. [19,20] presented upper limb and finger static balanced exoskeletons that used springs for movement assistance; Grazi et al. [21] presented an arm exoskeleton that assisted workers to better manage job tasks. Zhou et al. [22] presented a lower limb exoskeleton to assist walking; Eguchi et al. [23] presented a leg exoskeleton for upright locomotion; Hidayah [24] presented a knee exoskeleton that can do squats. Nguyen et al. [25,26] presented a robot arm that used gear-spring and delta parallel robot with static balance; Woo et al. [27] presented a static balanced surgical platform that used counterweight and springs for variable payloads. Martini et al. [28] presented indicators of joint reaction force and joint moment, which are helpful in evaluating different spring installation configurations. The static balance method using springs offers some merits, and de Vries et al. [29] presented an experiment on passive supporting upper limb exoskeleton to help workers doing plastering tasks. The exoskeleton is compact, and its weight is lighter than exoskeleton using motor to drive. Gosselin [30] presented an experiment on how manipulators with springs bring higher motor efficiency than manipulators without springs. Chiang and Chen [31] introduced a statically balanced manipulator with spring installation that can be easily adjusted and used for changeable payload. Nguyen et al. [32] proposed that static balancing can improve motion reliability of the mechanism. However, previous works mostly

[1]Corresponding author.

Contributed by the Mechanisms and Robotics Committee of ASME for publication in the Journal of Mechanisms and Robotics. Manuscript received August 20, 2022; final manuscript received February 14, 2023; published online March 8, 2023. Assoc. Editor: Stephen Canfield.

focused on how to reach static balance for manipulators or in other particular cases.

Gu et al. [33] displayed a fully coupled elastohydrodynamic model for the static performance analysis of gas foil bearings. Lee et al. [34] presented the effect of joint friction force on static performance of foil journal bearings. It is shown that larger joint reaction force makes higher pressure or friction on bearings, and thus lower static performance. Nguyen and Ahn [35] showed that the vibration of the system base of a linear motor motion stage can be significantly reduced with the reaction force compensation mechanisms. Seo [36] presented an effective designed reaction force compensator to inhibit vibration from the previous stages using laser direct imaging process. It can be seen that less reaction force would reduce the vibration effect on machines. Li and Lee [37] presented the effect of horizontal reaction force on the deflection of supported beams under transverse loadings. There are some advantages of the manipulator with a lower reaction force. For instance, Cocuzza et al. [38] claimed that the service life of a manipulator may be shorter than a manipulator under smaller reaction force. Li-Xin and Yong-Gang [39] presented that the dynamic performance of a planar 2-degrees-of-freedom (DOFs) pick-and-place parallel manipulator would be enhanced by a lower joint reaction force. It shows that a larger joint reaction force would increase friction force when the joint rotates or moves. De Luca [40] showed that a manipulator could be compact under small enough joint reaction force. Furthermore, it may also increase deflection on the end effector of the manipulator. Accordingly, with smaller joint reaction forces, lighter manipulators can be designed. Based on the aforementioned discussions, it is shown that joint reaction forces affect static and dynamic performance significantly. It is therefore necessary to investigate the joint reaction forces for a spring static balanced manipulator.

In this article, the formulation is used for a planar serial connected manipulator only, and the perfect static balance is achieved for the manipulator. The structure of this article is as follows. In Sec. 2, the variation of direction and elongation of spring is described. The representation of spring forces and joint re-action forces on a typical link of a static balanced n-link manipulator with only revolute joints is derived. Section 3 derives formulas of torque contributions that are affected by gravity, spring forces, and joint reaction force, with respect to the preconnected joint of a typical link that can be represented as a function of accumulative joint angle of links. In Sec. 4, the determination of spring attachment parameters (stiffness and attached lengths) is based on compatibility between gravitational torque and springs under static balanced conditions. Section 5 offers illustrative examples of two static balanced 3-DOF manipulators, in which one has springs and the other does not. It shows the reduction effect of joint reaction forces affected by spring forces at each link. The merits for the statically balanced manipulator from lower joint reaction force are presented. Finally, Sec. 6 provides the conclusion.

2 Spring Forces Representation of a Typical Link

Consider a single-link manipulator connected with a revolute joint at joint rotation angle 45 deg and 150 deg, as shown in Fig. 1, and that a zero-free-length spring is achieved by a cable and a pulley. Therefore, two ends of the spring can be regarded as connecting to the ground link and link 2 with zero-free-length characteristic. The direction and magnitude of the spring force can be affected by joint rotation angle and spring-attached parameters, which refer to spring stiffness and attached angles/lengths. With an uncertain spring attachment configuration, we cannot determine the spring force, as well as the joint reaction force on the preconnected joint of the link.

Consider a serially connected n-link manipulator, as shown in Fig. 2, where all the links are postconnected and preconnected with a revolute joint only. It would be assumed that the mass center of the link is in the middle location. For a typical link as

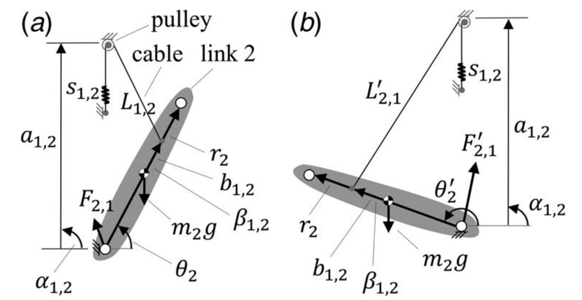

Fig. 1 A single-link manipulator with a zero-free-length spring at joint rotation angle of link 2: (a) 45 deg and (b) 150 deg

shown as link j $(2 \le j \le n)$, it is attached by a preconnecting spring, whose both ends are connected to link i and link j $(2 \le i < j)$, and known as $s_{i,j}$, and a postconnecting spring, which is connected to link j and link k $(j < k \le n)$, and known as $s_{j,k}$. Springs are arranged to a zero-free-length condition by cables and pulleys. There are two assumptions for springs: first, springs are zero-free-length and they are always in tension; second, there should be at most one spring attached between two distinct links.

Spring force can be defined by the product of stiffness and vector of elongation of the spring. As shown in Fig. 2, the vector of elongation of the preconnecting spring, $L_{i,j}$, is formed by three components: the attached vector of spring on link i and link j, and the vector of links that is crossed by spring. The vector of elongation of the spring can be expressed as follows:

$$L_{i,j} = a_{i,j}T(\Theta_{1,i} + \alpha_{i,j}) - \sum_{q=i+1}^{j-1} r_q T(\Theta_{1,q}) - b_{i,j}T(\Theta_{1,j} + \beta_{i,j}) \tag{1}$$

A spring-attached vector is presented as function of the spring-attached angles and spring-attached lengths, and the link vector is presented as function of an accumulative joint angle with respect to the ground and link length. In Eq. (1), $T(\Theta_{1,q})$ is the matrix of the transferring coordinate system of link q to the coordinate system of ground link; it can be expressed as follows:

$$T(\Theta_{1,q}) = \begin{bmatrix} \cos\Theta_{1,q} & -\sin\Theta_{1,q} \\ \sin\Theta_{1,q} & \cos\Theta_{1,q} \end{bmatrix} \tag{2}$$

The accumulative joint angle, $\Theta_{1,q}$, is summation of joint angles from joints between ground link and link q. As for the postconnecting spring of link j, $s_{j,k}$, its elongation is also represented by the vector of elongation of the preconnecting spring of link k with the opposite direction.

Figure 3 shows the free-body diagram of the manipulator; on the typical link, link j, it is acted by gravity force, preconnecting spring

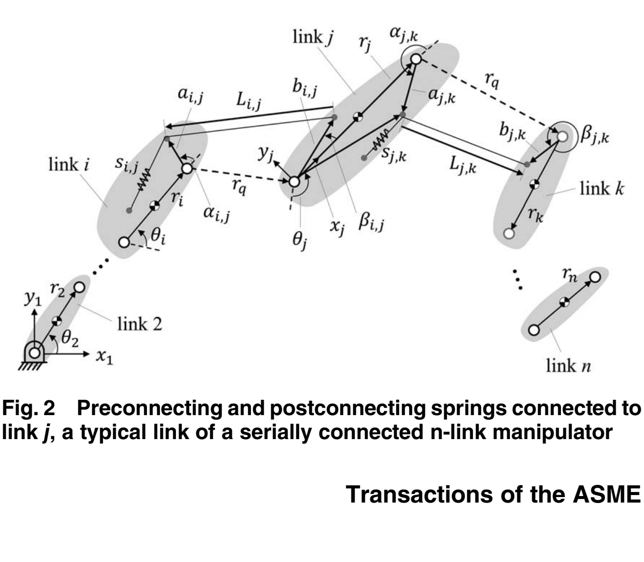

Fig. 2 Preconnecting and postconnecting springs connected to link *j*, a typical link of a serially connected n-link manipulator

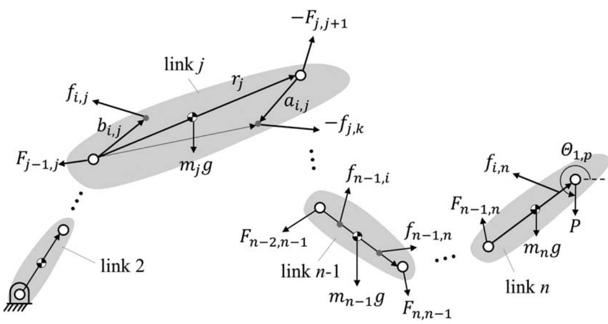

Fig. 3 Free-body diagram of a serially connected n-link manipulator

force, postconnecting spring force, reaction force, and external applied force.

The preconnecting spring force of link j, $f_{i,j}$, which is from the attached point of the spring on link j to another one on link i, can be expressed as follows:

$$\begin{aligned} f_{i,j} &= k_{i,j} L_{i,j} \\ &= k_{i,j}\left[a_{i,j} T(\Theta_{1,i} + \alpha_{i,j}) - \sum_{q=i+1}^{j-1} r_q T(\Theta_{1,q}) - b_{i,j} T(\Theta_{1,j} + \beta_{i,j}) \right] \end{aligned} \quad (3)$$

The postconnecting spring force of link j, $f_{k,j}$, can be presented as the preconnecting spring force of link k, $f_{j,k}$, with an opposite direction. Based on Eq. (1), the vector of elongation of the preconnecting spring of link k, and also the postconnecting spring force, can be expressed as follows:

$$\begin{aligned} f_{k,j} &= -f_{j,k} = -k_{j,k} L_{j,k} \\ &= -k_{j,k}\left[a_{j,k} T(\Theta_{1,j} + \alpha_{j,k}) - \sum_{q=j+1}^{k-1} r_q T(\Theta_{1,q}) - b_{j,k} T(\Theta_{1,k} + \beta_{j,k}) \right] \end{aligned} \quad (4)$$

The effect of joint reaction force on preconnected joint of link j, $F_{j-1,j}$, can be presented as the function of gravity force, spring forces, and external applied force on postconnected joint of the link. For the joint connected to the ground, its joint reaction force means base reaction force. The joint reaction force on the preconnected joint of link j can be expressed as follows:

$$F_{j-1,j} = -m_j g - \sum_{i=1}^{j-1} f_{i,j} - \sum_{k=j+1}^{n} f_{k,j} - FF_{j+1,j} \quad (5)$$

In Eq. (5), the external applied force, $F_{j+1,j}$, can be presented as joint reaction force on the preconnected joint of link $j+1$ with an opposite direction. The joint reaction force on the preconnected joint of link $j+1$, $F_{j,j+1}$, based on Eq. (5), can be expressed as follows:

$$F_{j,j+1} = -m_{j+1} g T(270 \text{ deg}) - \sum_{i=1}^{j} f_{i,j+1} + \sum_{k=j+2}^{n} f_{j+1,k} + F_{j+1,j+2} \quad (6a)$$

The same representation goes with link $j+2$ to link n; here, the joint reaction force on the preconnected joint of link n is shown as an example:

$$F_{n-1,n} = -m_n g T(270 \text{ deg}) - \sum_{i=1}^{n-1} f_{i,n} + \sum_{k=n+1}^{n} f_{n,k} + F_{n,n+1} \quad (6b)$$

Writing Eq. 6(a) by recursively substituting joint reaction force into external applied force for $n(j+1)$ times, the equation can be rewritten as follows:

$$F_{j,j+1} = -\sum_{k=j+1}^{n} \left(m_k g T(270 \text{ deg}) + \sum_{i=1}^{k-1} f_{i,k} - \sum_{v=j+1}^{k-1} f_{v,k} \right) + F_{n,n+1} \quad (7)$$

The first summation comes from link $j+1$ to link n for gravity, preconnecting spring forces, and postconnecting spring forces. The force on the postconnected joint of link n, $F_{n,n+1}$, is a payload with the opposite sign. The preconnecting spring forces, $f_{i,k}$, can be divided into three parts as follows:

$$\sum_{i=1}^{k-1} f_{i,k} = \sum_{i=1}^{j-1} f_{i,k} + f_{j,k} + \sum_{v=j+1}^{k-1} f_{v,k} \quad (8)$$

Substituting Eq. (8) into Eq. (7) yields

$$F_{j,j+1} = -\sum_{k=j+1}^{n} \left(m_k g[270 \text{ deg}] + \sum_{i=1}^{j-1} f_{i,k} + f_{j,k} + \text{P} \, [270 \text{ deg}] \right) \quad (9)$$

By substituting Eq. (9) into Eq. (5), the joint reaction force on preconnecting joint of link j is presented as functions of gravity, spring forces, and payload.

3 Torque Contributions of Springs Regarding Preconnecting Joint of a Typical Link

Torques acting on the preconnected joint of link j are caused by the force acting on the link. As shown in Fig. 3, the position vector of gravity is half of the vector of link j, and the torque caused by gravity in the preconnected joint of link j can be expressed as follows:

$$\tau_{1,j}^{g} = \frac{1}{2} r_j[\Theta_{1,j}] \times m_j g T(270 \text{ deg}) = -\frac{1}{2} r_j m_j g \sin(\Theta_{1,j} - 270 \text{ deg}) \quad (10)$$

Equation (10) shows that the torque caused by gravity is the function of accumulative joint angle $\Theta_{1,j}$ with coefficient. Figure 3 shows the position vector of preconnecting spring force, which acts on link j and is the postattached vector of the preconnecting spring on link j. According to Eq. (3), the torque caused by preconnecting spring forces can be expressed as follows:

$$\sum_{i=1}^{j-1} \tau_{i,j}^{s} = b_{i,j} T(\Theta_{1,j} + \beta_{i,j}) \times \sum_{i=1}^{j-1} f_{i,j} = \sum_{i=1}^{j-1} \left[-(kab)_{i,j} \sin(\Theta_{i,j} + (\beta_{i,j} - \alpha_{i,j})) + (kb)_{i,j} \sum_{q=i+1}^{j-1} r_q \sin(\Theta_{q,j} + \beta_{i,j}) \right] \quad (11)$$

The terms on the right-hand side of Eq. (11) are rearranged by separating the first torque contribution as a term with accumulative joint angle $\Theta_{1,j}$, and torques with the accumulative joint angle $\Theta_{2,j}$ to $\Theta_{j-1,j}$ are left. Combining the left torques with the second torque contribution, and replacing q and i with each other, the equation can then be rewritten as follows:

$$\sum_{i=1}^{j-1}\tau_{i,j}^{s}=-(kab)_{1,j}\sin(\Theta_{1,j}+(\beta_{1,j}-\alpha_{1,j}))+\sum_{i=2}^{j-1}\left[-(kab)_{i,j}\sin(\Theta_{i,j}+(\beta_{i,j}-\alpha_{i,j}))+\sum_{q=1}^{i-1}(kb)_{q,j}r_i\sin(\Theta_{i,j}+\beta_{q,j})\right] \tag{12}$$

Equation (12) shows that the torque caused by preconnecting spring force on preconnecting joint of link j is a function of accumulative joint angles $\Theta_{1,j}$ and $\Theta_{i,j}$ (form $\Theta_{2,j}$ to $\Theta_{j-1,j}$).

Figure 3 shows that the position vector of postconnecting spring force, $f_{j,k}$, that acts on link j is the sum of the vector of link j and the preattached vector of the postconnecting spring on link j. The torque caused by spring force can be expressed as follows:

$$\sum_{k=j+1}^{n}\tau_{j,k}^{s}=(r_jT(\Theta_{1,j})+a_{j,k}T(\Theta_{1,j}+\alpha_{j,k}))\times\sum_{k=j+1}^{n}(-f_{j,k})=r_jT(\Theta_{1,j})\times\sum_{k=j+1}^{n}(-f_{j,k})$$
$$+\sum_{k=j+1}^{n}\left[(kab)_{j,k}\sin(\Theta_{j,k}+(\alpha_{j,k}-\beta_{j,k}))+(ka)_{j,k}\sum_{v=j+1}^{k-1}r_v\sin(\Theta_{j,v}+\alpha_{j,k})\right] \tag{13}$$

Rearranging the terms on the right-hand side of Eq. (13) by combining the second torque contribution with the third torque contribution, and by replacing v and k with each other, the equation can be rewritten as follows:

$$\sum_{k=j+1}^{n}\tau_{j.k}^{s}=T(\Theta_{1,j})\times\sum_{k=j+1}^{n}(-f_{j,k})+\sum_{k=j+1}^{n}\begin{bmatrix}(kab)_{j,k}\sin(\Theta_{j,k}+(\beta_{j,k}-\alpha_{j,k}))\\+\sum\limits_{v=j+1}^{k-1}(ka)_{j,v}r_k\sin(\Theta_{j,k}-\alpha_{j,v})\end{bmatrix} \tag{14}$$

Equation (14) shows that the torque caused by postconnecting springs that acts on the preconnecting joint of link j is a function of accumulative joint angle $\Theta_{j,k}$ (from $\Theta_{j,j+1}$ to $\Theta_{j,n}$). Figure 3 shows that the position vector of external applied force, $F_{j+1,j}$, that acts on link j is the vector of link j. According to Eq. (9), the torque caused by external applied force can be expressed as follows:

$$\tau_{j,j+1}^{e}=r_jT(\Theta_{1,j})\times-F_{j,j+1}=r_jT(\Theta_{1,j})\times\sum_{k=j+1}^{n}\left(m_kgT(270\text{ deg})+\sum_{i=1}^{j-1}f_{i,k}+f_{j,k}+PT(270\text{ deg})\right) \tag{15}$$

External applied force is a function of gravity, spring force, and payload. It should be noted that the direction of the payload, P, is parallel to the direction of gravity. Based on Eqs. (10), (12), and (14), the torque caused by the external applied force can be rewritten as follows:

$$\tau_{j,j+1}^{e}=\sum_{k=j+1}^{n}\left\{\begin{array}{l}-r_j(m_kg+P)\sin(\Theta_{1,j}-270\text{ deg})-(ka)_{1,k}r_j\sin(\Theta_{1,j}-\alpha_{i,k})\\+\sum\limits_{i=2}^{j-1}\left[-(ka)_{i,k}r_j\sin(\Theta_{i,j}-\alpha_{i,k})+\sum\limits_{q=1}^{i-1}k_{q,k}r_ir_j\sin(\Theta_{i,j})\right]+r_j[\Theta_{1,j}]\times f_{j,k}\\-\sum\limits_{i=1}^{j-1}\left[(kb)_{i,k}r_j\sin(\Theta_{j,k}+\beta_{i,k})+\sum\limits_{v=j+1}^{k-1}k_{i,v}r_kr_j\sin(\Theta_{j,k})\right]\end{array}\right\} \tag{16}$$

Equation (16) shows that the torque is a function of accumulative joint angles $\Theta_{1,j}$, $\Theta_{i,j}$, and $\Theta_{j,k}$.

4 Torque Compatibilities Associated With Accumulative Joint Angles

For a statically balanced manipulator, the torque acting on the preconnected joint of each link will be in an equilibrium state. The torque equilibrium of link j can be expressed as follows:

$$\tau_{1,j}^{g}+\sum_{i=1}^{j-1}\tau_{i,j}^{s}+\sum_{k=j+1}^{n}\tau_{j.k}^{s}+\tau_{j,j+1}^{e}=0 \tag{17}$$

Torques can only cancel each other if they have the same phase. Hence, Eq. (17) does not entirely show the statically balanced condition, while the torques caused by different forces have different phases. Substituting Eqs. (10), (12), and (14) into Eq. (17), and collecting torques associated with accumulative joint angle $\Theta_{1,j}$, $\Theta_{2,j}$ to $\Theta_{j-1,j}$, and $\Theta_{j,j+1}$ to $\Theta_{j,n}$, torque equilibrium shown in Eq. (17) can be distinguished as three equations and expressed as follows:

$$\begin{aligned}&-r_j\left(\frac{1}{2}m_jg+m_kg+P\right)\sin(\Theta_{1,j}-270\text{ deg})\\&-(kab)_{1,j}\sin(\Theta_{1,j}+(\beta_{1,j}-\alpha_{1,j}))\\&-\sum_{k=j+1}^{n}(ka)_{1,k}r_j\sin(\Theta_{1,j}-\alpha_{1,k})=0\quad\text{for } j=2\ldots n\end{aligned} \tag{18}$$

$$\begin{aligned}&-(kab)_{i,j}\sin(\Theta_{i,j}+(\beta_{i,j}-\alpha_{i,j}))+(kb)_{1,j}r_i\sin(\Theta_{i,j}+\beta_{1,j})\\&+\sum_{q=2}^{i-1}(kb)_{q,j}r_i\sin(\Theta_{i,j}+\beta_{q,j})-\sum_{v=j+1}^{n}(ka)_{i,v}r_j\sin(\Theta_{i,j}-\alpha_{i,v})\\&+k_{1,v}r_ir_j\sin(\Theta_{i,j})+k_{q,v}r_ir_j\sin(\Theta_{i,j})=0\\&\text{for } j=2\ldots n \text{ and for } i=2\ldots j-1\end{aligned} \tag{19}$$

$$\begin{aligned}&(kab)_{j,k}\sin(\Theta_{j,k}+(\beta_{j,k}-\alpha_{j,k}))-\sum_{q=1}^{j-1}(kb)_{q,k}r_j\sin(\Theta_{j,k}+\beta_{q,k})\\&+\sum_{v=j+1}^{k-1}(ka)_{j,v}r_k\sin(\Theta_{j,k}-\alpha_{j,v})-k_{i,v}r_jr_k\sin(\Theta_{j,k})=0\\&\text{for } j=2\ldots n \text{ and for } k=j+1\ldots n\end{aligned} \tag{20}$$

For link j, comparing Eqs. (19) and (20), the coefficient in the sin function for both torques is the same, but the accumulative joint angles $\Theta_{i,j}$ and $\Theta_{j,k}$ are different. However, when a number ranging from 2 to n is brought into j, the accumulative joint angles $\Theta_{i,j}$ and $\Theta_{j,k}$ will be repeated. For example, when j equals 3 and i equals 2 in Eq. (19), it overlaps with j equals 2 and k equals 3 in Eq. (20). In accordance, this article only discusses Eqs. (18) and (19). By Ref. [41], the preattached angle and postattached angle of ground-attached springs are 90 deg and 0 deg, respectively, which can be expressed as follows:

$$\alpha_{1,j}=90\text{ deg}\quad\text{for } j=2\ldots n \tag{21a}$$

$$\beta_{1,j} = 0 \text{ deg} \quad \text{for } j = 2 \ldots n \tag{21b}$$

The preattached angle and postattached angle of non-ground-attached springs are 180 deg and 180 deg, respectively; which can be expressed as follows:

$$\alpha_{i,j} = 180 \text{ deg} \quad \text{for } j = 2 \ldots n \text{ and for } i = 2 \ldots j-1 \tag{22a}$$

$$\beta_{i,j} = 180 \text{ deg} \quad \text{for } j = 2 \ldots n \text{ and for } i = 2 \ldots j-1 \tag{22b}$$

Substituting Eqs. (21*a*), (21*b*), and (22*a*)–(22*b*) into Eqs. (18) and (19), the coefficient compatibility between gravity and springs can be formulated as follows:

$$(kab)_{1,j} + \sum_{k=j+1}^{n} (ka)_{1,k} r_j = r_j \left(\frac{1}{2} m_j g + m_k g + P \right) \quad \text{for } j = 2 \ldots n \tag{23}$$

$$-(kab)_{i,j} + (kb)_{1,j} r_i + \sum_{q=2}^{i-1} (kb)_{q,j} r_i - \sum_{v=j+1}^{n} (ka)_{i,v} r_j + \sum_{q=1}^{i-1} k_{q,v} r_i r_j = 0$$
$$\text{for } j = 2 \ldots n \text{ and for } i = 2 \ldots j-1 \tag{24}$$

Noted that, the stiffness and attached length of springs cannot be negative numbers in the framework of this article. Based on Eq. (23), given the link properties, coefficient compatibility with the accumulative joint angle between ground-attached springs can be obtained. The order of selecting the attachment parameters of ground-attached springs is from the spring with a large number of bridging to the spring with a small number of bridging. Based on Eq. (24), after selecting the attachment parameters of ground-attached springs, the order of selecting attachment parameters of non-ground-attached springs can also be carried out in the same manner, which is from the spring with a large number of bridging to the spring with a small number of bridging. In this way, the attachment parameters of springs that are in statically balanced conditions are selected by coefficient compatibility.

After choosing a set of solutions for stiffness and attached length of springs with the known attached angle of springs, the direction and elongation of spring force are mere functions of accumulative joint angles, which means that the spring force is then known. Based on Eq. (8), reaction force that acts on preconnected joint of links can be formulated with only accumulative joint angles and can be determined inwardly from end link of the manipulator as the process of robotics.

5 Illustrative Examples: A Statically Balanced 3 Degrees-of-Freedom Manipulator

A statically balanced 3-DOF manipulator without springs is shown in Fig. 4(*a*); the manipulator that has four springs, $s_{1,2}$, $s_{1,4}$, $s_{2,3}$, and $s_{2,4}$, is shown in Fig. 4(*b*). These springs are connected to the ground link and are arranged by cable and pulley to let them pass through joint and the connected points of springs as zero-free-length springs [42]. Springs installed on the ground link have required space for their free-length and elongation. This method allows normal springs to achieve zero-free-length characteristic practically. The manipulator in both figures is at joint relative angles of link 2, link 3, and link 4, respectively, at 45 deg, 315 deg, and 280 deg. The attached angles and attached lengths of springs do not vary along with the movements of the manipulator. It is assumed that the mass values of links are 30, 26, and 18 (kg) and the lengths of links are 0.4, 0.35, and 0.3 (m) for link 2, link 3, and link 4, respectively, and the payload is assumed as 180 (N) in Table 1.

With the example, the stiffness and attached length of the ground-attached spring $s_{1,4}$ and $s_{1,2}$ based on Eq. (23) can be expressed as follows:

$$(kab)_{1,4} = r_4 \left(\frac{1}{2} m_4 g + P \right) = 80.5 \tag{25}$$

$$(ka)_{1,4} = \left(\frac{1}{2} m_3 g + m_4 g + P \right) = 483.8 \tag{26}$$

$$(kab)_{1,2} = r_2 \left(\frac{1}{2} m_2 g + m_3 g + m_4 g + P \right) - (ka)_{1,4} r_2 = 109.8 \tag{27}$$

Based on Eqs. (25)–(27), the postattachment length of spring $s_{1,4}$ is determined as 0.17 (m). Based on Eq. (26), it can be assumed that the preattached length is 1.1 (m), and the spring stiffness is 440.8 (N/m). Based on Eq. (27), it can be assumed that the preattached length and postattached length of spring $s_{1,2}$ are 0.7 and 0.2 (m), respectively, and the spring stiffness is 784.8 (N/m).

For non-ground-attached springs, $s_{2,4}$ and $s_{2,3}$, the selected spring parameters of ground-attached springs are substituted into Eq. (24), and their stiffness and attached lengths can be expressed as follows:

$$(kab)_{2,4} = (kb)_{1,4} r_2 = 29.6 \tag{28}$$

$$(kb)_{2,4} = (kb)_{1,4} = 74.9 \tag{29}$$

$$(kab)_{2,3} = k_{1,4} r_2 r_3 + k_{2,4} a_{2,4} r_3 = 95.9 \tag{30}$$

Based on Eqs. (28) and (30), the preattached length of spring $s_{2,4}$ is determined as 0.4 (m); assuming its postattached length is 0.3 (m),

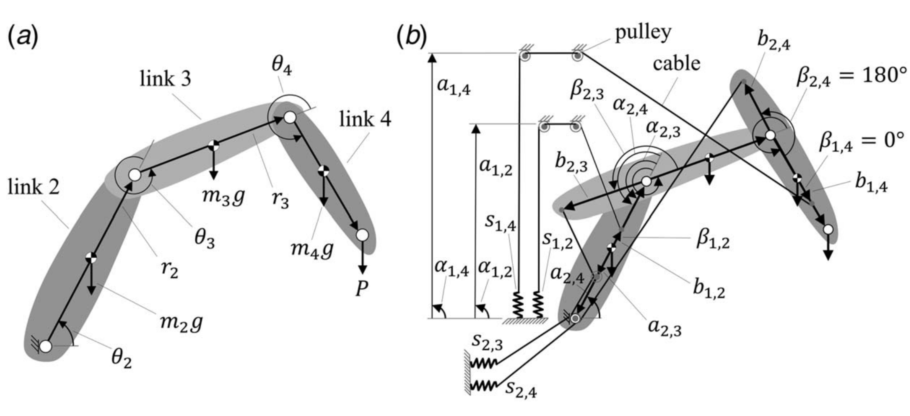

Fig. 4 3-DOF manipulators: (*a*) without springs and (*b*) with springs $s_{1,4}$, $s_{2,4}$, $s_{2,3}$, and $s_{1,2}$ (joint angle $\theta_2 = 45$ deg, $\theta_3 = 315$ deg, and $\theta_4 = 280$ deg)

Table 1 Mass and length of link 2, link 3, and link 4 of the 3-DOF manipulator

Link j	2	3	4
m_j (kg)	30	26	18
r_j (m)	0.4	0.35	0.3

Table 2 Attached length and stiffness of the springs $s_{1,4}$, $s_{1,2}$, $s_{2,4}$, and $s_{2,3}$

$s_{i,j}$	$s_{1,4}$	$s_{1,2}$	$s_{2,4}$	$s_{2,3}$
$a_{i,j}$ (m)	1.10	0.70	0.40	0.25
$b_{i,j}$ (m)	0.17	0.20	0.30	0.35
$k_{i,j}$ (N/m)	440.8	784.8	243.9	2554

and with reference to Eq. (29), its spring stiffness is then determined as 243.9 (N/m). Based on Eq. (30), it is assumed that the preattached length and postattached length of spring $s_{2,3}$ are 0.25 and 0.35 (m), respectively; its spring stiffness is then determined as 2554 (N/m). The attached lengths of springs are shown in Table 2.

With determined spring-attached parameters, joint reaction force can be determined by investigating the effect of spring forces on joint reaction forces. Substituting link parameters and spring-attached parameters into Eq. (3), and then substituting its outcome into Eq. (9), the reaction force on the preconnected joint of link 4, link 3, and link 2 can be expressed as follows:

$$F_{3,4} = -356.6[270\ \text{deg}] - (484.1[90\ \text{deg}] - 176.3[\Theta_{2,1}] - 154.3[\Theta_{3,1}]) \tag{31}$$

$$F_{2,3} = -611.6[270\ \text{deg}] - (484.1[90\ \text{deg}] - 238.6[\Theta_{2,1}] + 242.2[\Theta_{3,1}]) \tag{32}$$

$$F_{1,2} = -905.9[270\ \text{deg}] - (1033.5[90\ \text{deg}] - 133.1[\Theta_{2,1}] - 128.9[\Theta_{3,1}]) \tag{33}$$

From Eqs. (31)–(33), it can be seen that the gravity force does not vary along the movements of the accumulated joint angles. On the contrary, unlike gravity force, the torque contribution caused by springs varies due to the different postures of the manipulator. Assuming the range of motion as θ_2:0 deg–90 deg, θ_3: −90 deg–90 deg, and θ_4:0–360 deg, and substituting them into Eqs. (31)–(33), the spring forces of the manipulator with gravity balance can be obtained as the terms in the parentheses shown in Fig. 5.

The joint reaction forces of the manipulator with gravity balance can be acquired as shown in Fig. 6. As for the manipulator without springs but has massless motors installed to maintain statically balanced condition, the joint reaction force on the preconnected joint of links would be caused only by gravity. According to Eqs. (30)–(32), the joint reaction force is the first term, which is associated to 270 deg only, as shown in Fig. 6. From the global coordinated system's perspective, the joint reaction force does not vary along the different postures of links.

During the motion of the manipulator, the percentage of area for decreased reaction force can be obtained by dividing the amount of data of reduced reaction forces by the total amount of data. For example, the percentage of reaction force with spring forces is similarly about 100% for link 4, link 3, and link 2. Comparing the variation of root-mean-square (RMS) of the reaction force with springs to those without springs, each link has decreased by 34.5%, 34.5%, and 68.4%, respectively. Hence, the reaction force on each link is not optimized with spring stiffness or attached lengths. This 3-DOF manipulator with springs is an example that shows the determination of spring-attached parameters and the variation of reaction force. Therefore, this result merely shows the potential ability of spring forces in reducing joint reaction forces. The joint reaction forces may be entirely reduced through some spring installation configurations. In this study, the result shows the difference of joint reaction force between manipulator with springs and without

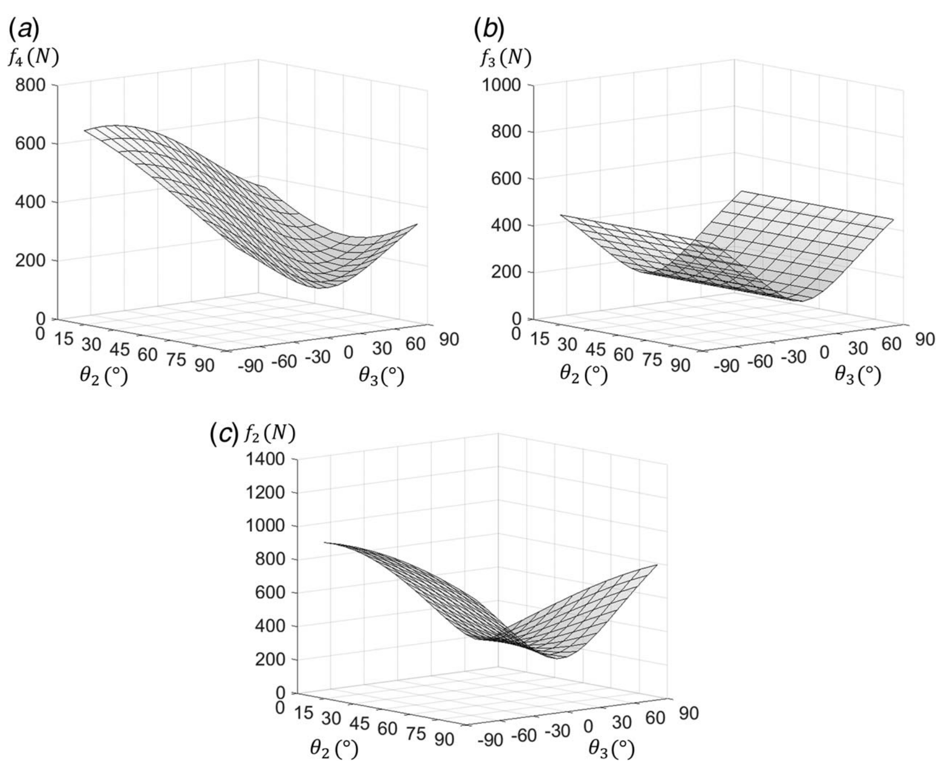

Fig. 5 Spring force of a 3-DOF manipulator with gravity balance in a range of motion: magnitude of spring force on (*a*) link 4, (*b*) link 3, and (*c*) link 2

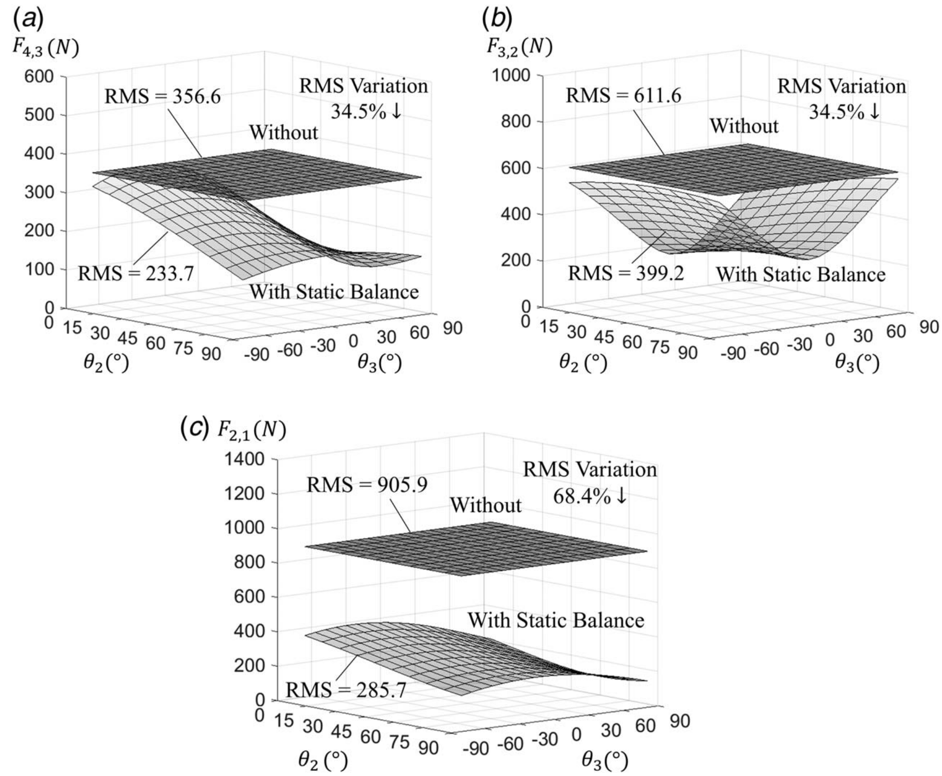

Fig. 6 Joint reaction force of a 3-DOF manipulator with/without static balance in a range of motion: magnitude of reaction force on (*a*) link 4, (*b*) link 3, and (*c*) link 2

springs in achieving static balance. Definitely, there are other sets of spring-attached parameters that can reach static balance. However, which of these sets of solutions best optimizes joint reaction force and leads to the best spring attached installation is not the main purpose of this article. By reducing joint reaction force, the manipulator could reach the same purpose with lower strength of joints and links. Based on using more compact links, it makes the weight of manipulator lighter and the life expectancy of joints longer by lower joint reaction force.

6 Conclusions

This article presents the analysis of joint reaction forces by spring attachment parameters determination based on torque compatibility under statically balanced conditions. While torques on each joint caused by gravity, spring force, and external applied force in terms of accumulated joint angles maintain equilibrium, the compatibility of the stiffness, attached lengths of springs can be obtained with the given spring-attached angles. The postattached length of ground-attached springs is therefore determined, and the product of its stiffness and preattached length is equal to constant. The spring stiffness and attached lengths of non-ground-attached springs are constrained by the stiffness and postattached length of ground-attached springs. With designed spring-attached parameters, joint reaction force can be determined inwardly from the end link. In the example of the 3-DOF statically balanced manipulator, the comparison of joint reaction forces between manipulators with and without springs shows that these forces are normally reduced by the effect of springs. Reduced joint reaction forces offer benefits such as creating lower friction force on joints, and reducing deflection on the end-point of a robot arm. Furthermore, the manipulator with lightweight links, that is, with less strength, can be used for lower reaction forces. This research proposed another consideration for the design of statically balanced serially connected manipulators.

Funding Data

- The Ministry of Science and Technology (MOST) (Grant No. 109-2221-E-002-002-MY3).

Conflict of Interest

There are no conflicts of interest.

Data Availability Statement

The authors attest that all data for this study are included in the paper.

Nomenclature

g = value of gravitational acceleration
P = payload on end link of manipulator
$a_{i,j}$ = preattached length of position vector of spring on link i from postconnecting joint to attached point of spring on link i
$b_{i,j}$ = postattached length of position vector of spring on link j from preconnecting joint to attached point of spring on link j
$f_{i,j}$ = spring force from attached point of spring on link j to attached point of spring on link i
$k_{i,j}$ = spring stiffness
m_j = mass of link j
r_j = length from preconnecting joint to postconnecting joint of link j
$s_{i,j}$ = a spring attached to link i and link j
x_j = X-axis vector of coordinate system of link j
y_j = Y-axis vector of coordinate system of link j
$F_{j-1,j}$ = reaction force on preconnecting joint of link j by link j 1

$L_{i,j}$ = elongation of spring from attached point of spring on link j to attached point of spring on link i
$\alpha_{i,j}$ = preattached angle of the spring from x_i axis of link i to position vector of spring on link i
$\beta_{i,j}$ = postattached angle of spring from x_i axis of link j to position vector of spring on link j
θ_j = angle from x_{j-1} axis to x_j axis
$\Theta_{i,j}$ = accumulated angle from x_{i+1} to axis to x_j axis
$\tau^g_{1,j}$ = torque caused by gravity force of link j with respect to preconnecting joint of link j
$\tau^s_{i,j}$ = torque caused by preconnecting spring with respect to preconnecting joint of link j
$\tau^s_{j,k}$ = torque caused by postconnecting spring with respect to preconnecting joint of link j
$\tau^r_{j+1,j}$ = torque caused by external applied force acting on postconnecting joint of link j with respect to preconnecting joint of link j

References

[1] Salisbury, J., and Craig, J., 1982, "Articulated Hands: Kinematic and Force Control Issues," Int. J. Robot. Res., **1**(1), pp. 4–17.
[2] Orin, D. E., McGhee, R. B., Vukobratović, M., and Hartoch, G., 1979, "Kinematic and Kinetic Analysis of Open-Chain Linkages Utilizing Newton-Euler Methods," Math. Biosci., **43**(1–2), pp. 107–130.
[3] Baker, D. R., and Wampler, C. W., 1988, "On the Inverse Kinematics of Redundant Manipulators," Int. J Robot. Res., **7**(2), pp. 3–21.
[4] Aversa, R., Petrescu, R. V. V., Akash, B., Bucinell, R. B., Corchado, J. M., Berto, F., Mirsayar, M., et al., 2017, "Kinematics and Forces to a New Model Forging Manipulator," Am. J. Appl. Sci., **14**(1), pp. 60–80.
[5] Suarez, A., Jimenez-Cano, A. E., Vega, V. M., Heredia, G., Rodriguez-Castaño, A., and Ollero, A., 2018, "Design of a Lightweight Dual arm System for Aerial Manipulation," Mechatronics, **50**(1), pp. 30–44.
[6] Hockstein, N. G., Nolan, J. P., O'Malley, B. W., and Woo, Y. J., 2005, "Robotic Microlaryngeal Surgery: a Technical Feasibility Study Using the DaVinci Surgical Robot and an Airway Mannequin," Laryngoscope, **115**(5), pp. 780–785.
[7] Wang, W., Li, J., Wang, S., Su, H., and Jiang, X., 2016, "System Design and Animal Experiment Study of a Novel Minimally Invasive Surgical Robot," Int. J. Med. Robot. Comp., **12**(1), pp. 73–84.
[8] Yamamoto, T., Terada, K., Ochiai, A., Saito, F., Asahara, Y., and Murase , K., 2019, "Development of Human Support Robot as the Research Platform of a Domestic Mobile Manipulator," Robomech. J., **6**(1), pp. 1–15.
[9] Otten, A., Voort, C., Stienen, A., Aarts, R., van Asseldonk, E., and van der Kooij, H., 2015, "LIMPACT: A Hydraulically Powered Self-Aligning Upper Limb Exoskeleton," IEEE/ASME Trans. Mech., **20**(5), pp. 2285–2298.
[10] Gopura, R., Bandara, D. S. V., Kiguchi, K., and Mann, G. K. I., 2016, "Developments in Hardware Systems of Active Upper-Limb Exoskeleton Robots: A Review," Robot. Auton. Syst., **75**(1), pp. 203–220.
[11] Deepak, S. R., and Ananthasuresh, G., 2009, "Static Balancing of Spring-Loaded Planar Revolute-Joint Linkages Without Auxiliary Links," 14th National Conference on Machines and Mechanisms, NIT, Durgapur, India, Dec. 17–18.
[12] Tschiersky, M., Hekman, E. E. G., Herder, J. L., Brouwer, D. M., and Tschiersky, M., 2021, "Gravity Balancing Flexure Spring Mechanisms for Shoulder Support in Assistive Orthoses," IEEE T. Med. Robot. Bio., **4**(2), pp. 448–459.
[13] Barents, R., Schenk, M., van Dorsser, W. D., Wisse, B. M., and Herder, J. L., 2011, "Spring-to-Spring Balancing as Energy-Free Adjustment Method in Gravity Equilibrators," ASME J. Mech. Des., **133**(6), p. 061010.
[14] Van Dorsser, W. D., Barents, R., Wisse, B. M., and Herder, J. L., 2007, "Gravity-Balanced Arm Support With Energy-Free Adjustment," ASME J. Med. Dev., **1**(2), pp. 151–158.
[15] Deepak, S. R., and Ananthasuresh, G., 2012, "Perfect Static Balance of Linkages by Addition of Springs but Not Auxiliary Bodies," ASME J. Mech. Rob., **4**(2), p. 021014.
[16] Lin, P.-Y., Shieh, W.-B., and Chen, D.-Z., 2009, "Design of Perfectly Statically Balanced One-DOF Planar Linkages With Revolute Joints Only," ASME J. Mech. Des., **131**(5), p. 051004.
[17] Lin, P.-Y., Shieh, W.-B., and Chen, D.-Z., 2011, "Design of Statically Balanced Planar Articulated Manipulators With Spring Suspension," IEEE T. Robot., **28**(1), pp. 12–21.
[18] Lee, Y.-Y., and Chen, D.-Z., 2014, "Determination of Spring Installation Configuration on Statically Balanced Planar Articulated Manipulators," Mech. Mach. Theory, **74**(1), pp. 319–336.
[19] Huysamen, K., Bosch, T., de Looze, M., Stadler, K. S., Graf, E., and O'Sullivan, L. W., 2018, "Evaluation of a Passive Exoskeleton for Static Upper Limb Activities," Appl. Ergon., **70**(1), pp. 148–155.
[20] Bortoletto, R., Mello, A. N., and Piovesan, D., 2017, "A Springs Actuated Finger Exoskeleton: From Mechanical Design to Spring Variables Evaluation," 2017 International Conference on Rehabilitation Robotics (ICORR), London, UK, July 17–20.
[21] Grazi, L., Trigili, E., Proface, G., Giovacchini, F., Crea, S., and Vitiello, N., 2020, "Design and Experimental Evaluation of a Semi-Passive Upper-Limb Exoskeleton for Workers With Motorized Tuning of Assistance," IEEE T. Neur. Sys. Reh., **28**(10), pp. 2276–2285.
[22] Zhou, L., Chen, W., Chen, W., Bai, S., Zhang, J., and Wang, J., 2020, "Design of a Passive Lower Limb Exoskeleton for Walking Assistance With Gravity Compensation," Mech. Mach. Theory, **150**(1), p. 103840.
[23] Eguchi, Y., Kadone, H., and Suzuki, K., 2018, "Standing Mobility Device With Passive Lower Limb Exoskeleton for Upright Locomotion," IEEE/ASME T. Mech., **23**(4), pp. 1608–1618.
[24] Hidayah, R., Sui, D., Wade, K. A., Chang, B.-C., and Agrawal, S., 2021, "Passive Knee Exoskeletons in Functional Tasks: Biomechanical Effects of a SpringExo Coil-Spring on Squats," Wear Technol., **2**(1), p. e7.
[25] Nguyen, V. L., Lin, C.-Y., and Kuo, C.-H., 2020, "Gravity Compensation Design of Planar Articulated Robotic Arms Using the Gear-Spring Modules," ASME J. Mech. Rob., **12**(3), p. 031014.
[26] Nguyen, V. L., Lin, C.-Y., and Kuo, C.-H., 2020, "Gravity Compensation Design of Delta Parallel Robots Using Gear-Spring Modules," Mech. Mach. Theory, **154**(1), p. 104046.
[27] Woo, J., Seo, J.-T., and Yi, B.-J., 2019, "A Static Balancing Method for Variable Payloads by Combination of a Counterweight and Spring and Its Application as a Surgical Platform," Appl. Sci., **9**(19), p. 3955.
[28] Martini, A., Troncossi, M., and Rivola, A., 2019, "Algorithm for the Static Balancing of Serial and Parallel Mechanisms Combining Counterweights and Springs: Generation, Assessment and Ranking of Effective Design Variants," Mech. Mach. Theory, **137**(1), pp. 336–354.
[29] de Vries, A. W., Krause, F., and de Looze, M. P., 2021, "The Effectivity of a Passive Arm Support Exoskeleton in Reducing Muscle Activation and Perceived Exertion During Plastering Activities," Ergonomics, **64**(6), pp. 712–721.
[30] Gosselin, C., 2008, "Gravity Compensation, Static Balancing and Dynamic Balancing of Parallel Mechanisms," *Smart Devices and Machines for Advanced Manufacturing*, L. Wang, and J. Xi, eds., Springer-Verlag Limited, London, pp. 27–48.
[31] Chiang, W.-H., and Chen, D.-Z., 2017, "Design of Planar Variable-Payload Balanced Articulated Manipulators With Actuated Linear Ground-Adjacent Adjustment," Mech. Mach. Theory, **109**(1), pp. 296–312.
[32] Nguyen, V. L., Kuo, C.-H., and Lin, P. T., 2022, "Reliability-Based Analysis and Optimization of the Gravity Balancing Performance of Spring-Articulated Serial Robots With Uncertainties," ASME J. Mech. Rob., **14**(3), p. 031016.
[33] Gu, Y., Ren, G., and Zhou, M., 2020, "A Fully Coupled Elastohydrodynamic Model for Static Performance Analysis of Gas Foil Bearings," Tribol. Int., **147**(1), p. 106297.
[34] Lee, D.-H., Kim, Y.-C., and Kim, K.-W., 2010, "The Effect of Coulomb Friction on the Static Performance of Foil Journal Bearings," Tribol. Int., **43**(5–6), pp. 1065–1072.
[35] Nguyen, D. C., and Ahn, H. J., 2014, "Dynamic Analysis and Iterative Design of a Passive Reaction Force Compensation Device for a Linear Motor Motion Stage," Int. J. of Precis. Eng. Man., **15**(11), pp. 2367–2373.
[36] Seo, C.-H., Jeon, Y. H., Lee, H.-K., Kim, H.-Y., and Lee, M. G., 2018, "Reaction Force Compensator for High-Speed Precision Stage of Laser Direct Imaging Process," Shock Vib., **2018**(1), p. 8324539.
[37] Li, X.-F., and Lee, K. Y., 2015, "Effect of Horizontal Reaction Force on the Deflection of Short Simply Supported Beams Under Transverse Loadings," Int. J. Mech. Sci., **99**(1), pp. 121–129.
[38] Cocuzza, S., Pretto, I., and Debei, S., 2011, "Novel Reaction Control Techniques for Redundant Space Manipulators: Theory and Simulated Microgravity Tests," Acta Astronaut., **68**(11–12), pp. 1712–1721.
[39] Li-Xin, X., and Yong-Gang, L., 2014, "Investigation of Joint Clearance Effects on the Dynamic Performance of a Planar 2-DOF Pick-and-Place Parallel Manipulator," Robot. Comput. Integr. Manuf., **30**(1), pp. 62–73.
[40] De Luca, A., Albu-Schaffer, A., Haddadin, S., and Hirzinger, G., 2006, "Collision Detection and Safe Reaction With the DLR-III Lightweight Manipulator Arm," 2006 IEEE/RSJ International Conference on Intelligent Robots and Systems, Beijing, China, Oct. 9–15.
[41] Juang, C.-W., and Chen, D.-Z., 2022, "Spring Configurations and Attachment Angles Determination for Statically Balanced Planar Articulated Manipulators," ASME J. Mech. Rob., **14**(5), p. 054502.
[42] Delissen, A. A., Radaelli, G., and Herder, J. L., 2017, "Design and Optimization of a General Planar Zero Free Length Spring," Mech. Mach. Theory, **117**(1), pp. 56–77.